

Light absorption enhancement in organic solar cell using non-concentric Ag:SiO₂ core-shell nanoparticles

Mulda Muldarisnur*, F. Fahendri, Ilham Perdana, Zulfi Abdullah, Meqorry Yusfi

Department of Physics, Faculty of Mathematics and Natural Sciences, Universitas Andalas, Padang 25163, Indonesia

Article history:

Received: 23 December 2022 / Received in revised form: 30 May 2023 / Accepted: 11 June 2023

Abstract

Low solar energy conversion efficiency prevents the widespread of organic solar cells; hence, metal nanoparticles have been used to overcome this problem without increasing cell thickness. We investigated light absorption enhancement in view of the embedment of Ag:SiO₂ core-shell nanoparticles of different shell thicknesses, core offsets, offset orientation angles, and vertical mismatches between neighboring particles. The simulations were carried out using the finite element method. This is the first investigation in the use of asymmetric nanoparticles. At optimized conditions, absorption enhancement up to 345% compared to the one without the nanoparticles could be achieved. The enhancement was found much higher than that of the published values. The enhancement results were mainly from the increase of near-field localization and scattering in the active layer of solar cells due to the excitation of Fano resonances. The resonance occurred due to the non-symmetric nature of the core-shell nanoparticles.

Keywords: Organic solar cell; absorption enhancement; core-shell nanoparticle; surface plasmon resonance; scattering

1. Introduction

Solar energy conversion will contribute significantly to energy production in the future. Since fossil fuels are rapidly depleting, fluctuating in price, and environmentally unfriendly, clean and renewable energy sources must be developed to fulfil the world's increasing energy demand. Compared to other renewable sources, solar energy is the most abundant, easily accessible, sustainable, and non-destructive. Significant obstacles to market penetration of solar cells are related to high production and installation cost, limited lifetime, or low efficiency.

Organic solar cells (OSCs) are promising alternatives to those inorganic-based cells due to their low cost, mechanical flexibility, semi-transparency, lightweight, and easy large-scale fabrication [1,2]. Moderate efficiency and relatively rapid photo-degradation, however, have restricted the spread of OSCs. The conjugated organic molecules that are used as active materials exhibit intense and broad absorption. However, their optimal use is prohibited due to the use of a very thin (commonly smaller than 100 nm) active layer [3–6]. The unabsorbed light escapes from the cell and does not contribute to photocurrent generation. Increasing the active layer thickness cannot be done due to low charge carrier mobility and short exciton diffusion length, which are caused by the hopping transport of electrons between the localized states of the conjugated polymer [7]. Thicker active material causes higher

recombination loss and fewer extracted charges. Low absorption implies the importance of light-trapping schemes [8,9]. Light trapping enables absorption enhancement by reducing light reflection at the interface and increasing the light path length inside the active layer. At a fixed physical thickness, the optical thickness of the active layer increases several times.

Several trapping mechanisms have been proposed, such as diffraction grating [10–12], photonic crystals [13,14], random scatterers [15], micro-lenses [16,17], or metal nanoparticles [18,19]. The mentioned structures enhance in coupling the efficiency of light and increase the effective propagation length of light in the active materials. As a result, the probability of light being absorbed by the active materials for generating excitons increases. The use of photonic structures is restricted by the relatively low refractive indices of organic materials and the active layer that is too thin to support the guided optical modes. Light focusing using micro-lenses depends sensitively on the position of the lenses; therefore, it is unsuitable for thin solar cells.

Metallic nanostructures offer a number of advantages such as light absorption enhancement without an increase in the thickness of OSCs. Metallic nanoparticles enhance light absorption through scattering or optical path length increase and local field enhancement. They have been embedded in the buffer layer, interface buffer-active layers, and active layers [20–23]. When nanoparticles are embedded in buffer layers, the enhancement is caused by enhanced forward scattering. In contrast, local field enhancement is more dominant when metal nanoparticles are located in the active layer. An enhanced electric field in the active layer generates more excitons within

* Corresponding author.

Email: muldarisnur@sci.unand.ac.id

<https://doi.org/10.21924/cst.8.1.2023.1076>

their diffusion length. The exact mechanism for light absorption enhancement depends on nanoparticle size, composition, shape, and position inside an OSC [24,25]. The use of bare metal nanoparticles in the active layer should be avoided considering that they may act as recombination center and cause exciton quenching [26,27]. Charge recombination and exciton quenching will become more severe for larger nanoparticles [28]. The negative effect of metal nanoparticles embedded in the active layer of OSC, however, can be eliminated by coating the particles using thin dielectric material [29-31]. Many synthesis methods for metallic [32] and core-shell [33] nanoparticles have been reported before.

Our previous work found that light absorption enhancement depends highly on the core particle's diameter and position within the organic solar cell [34]. Here, we aim to enhance light absorption further by investigating the effect of core offset, angular orientation of core offset, periodicity, and vertical position mismatch of Ag:SiO₂ core-shell nanoparticle on the absorption enhancement of OSC. The use of asymmetric core-shell nanoparticles allows the excitation of Fano resonances that is responsible for the further increase of localized electric field around the metal nanoparticles. Non-concentric nanoparticles result in a broadband absorption enhancement. We found an enhancement up to 345%, much higher than that of the reported data. We also showed the vital role of core-offset orientation angle and vertical mismatch in the position of neighboring nanoparticles on light absorption enhancement. These effects, so far, have not been reported in literature.

2. Materials and Methods

We used the finite element method [35,36] to calculate light absorption enhancement in the active layer of OSC. In this method, the OSC structure was divided into small volumetric meshes where the electric and magnetic fields were calculated at the nodes of each mesh. The finite element method converted partial differential Maxwell's equations into a set of algebraic equations arranged into a matrix form. The core-shell nanoparticles in this simulation were assumed to be arranged periodically in two lateral dimensions. The periodicity allowed the simulation of only one unit-cell consisting of a single core-shell particle. At the lateral boundaries of the unit cell, perfectly-match conditions are imposed to prevent non-physical reflection from reentering the simulation area. Total field and scattered field formulation were used in the vertical plane boundaries. An incoming plane wave with a unity power density was injected into the simulation region at a normal incidence.

We simulated a standard four-layer bulk heterojunction OSC consisting of transparent conductor ITO (indium tin oxide) as a cathode, PEDOT: PSS (poly 3,4-ethylenedioxythiophene: polystyrene sulfonate) as a hole transporting layer, P3HT:PCBM (poly3-hexylthiophene-phenyl-C6-butyric acid methyl ester) as an active layer for light absorption, and aluminum as an anode. The aluminum also served as a back reflector reflecting non-absorbed light from the active layer. The PEDOT: PSS layer is often used in experiments because it flattens the ITO surface, seals the active layer from oxygen, prevents the diffusion of the anode material into the active layer, enhances the cell mechanically, and eases the charge

extraction process. The P3HT is a p-type semiconductor polymer that absorbs visible light and has excellent delocalized electrons along the conjugated backbone. The P3HT and PCBM are commonly used as donor and acceptor materials in the photoactive layer for being commercially available and relatively stable for prolonged use. Light absorption creates excitons that diffuse inside the material before reaching the donor-acceptor interface. The formed electric field at the interface separates the excitons into free electrons and holes [37].

Figure 1 shows the thickness of each layer of organic OSC structure. PEDOT: PSS and P3HT: PCBM were at 20 nm and 50 nm, respectively. The diameter of the silver core was 40 nm, and the particle's position was fixed at 21 nm above the interface of the active layer and aluminum, resulting in the highest light absorption enhancement [34]. The thickness of the silica shell varied 1-4 nm, while the position of the silver core was shifted horizontally up to the maximum allowed offset (δ_{\max}) equal to the shell's thickness (t_{SiO_2}). Moreover, the angle of the core offset was varied from 0 - 360°. We also investigated the vertical position mismatch between neighboring Ag:SiO₂ particles. The light source was simulated as a plane wave source with a wavelength range from 350 nm to 700 nm propagating at a normal incident angle from air to the surface of OSC. Real and imaginary components of refractive indices data for all layers and nanoparticles were obtained from <http://www.refractiveindex.info> webpage and the solar radiation spectrum was obtained from standard data [38].

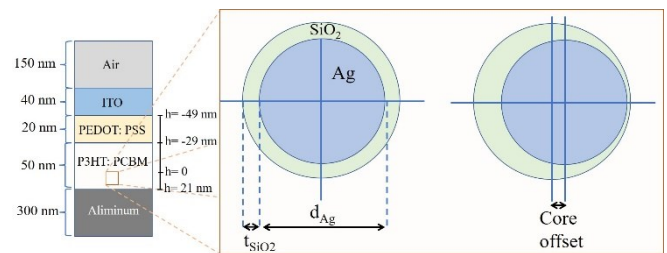


Fig. 1. (a) OSC structure, (b) embedded Ag:SiO₂ concentric core-shell nanoparticle, and (c) Ag:SiO₂ nanoparticle with an offset in the position of the core. (note: image is not to scale)

After solving Maxwell's equation using the finite element method, the dissipated power of the electromagnetic wave was calculated by performing the volume integration of the Poynting vector in the active layer. The absorption of the active layer of the OSC was defined as the ratio of the dissipated power to the incoming power from the source. The absorption enhancement due to the incorporation of core-shell nanoparticles was defined as the ratio of the total absorbed power over the investigated wavelength range with nanoparticles to the absorption without nanoparticles [29,30].

3. Results and Discussion

3.1. Effect of core offset

Figure 2 shows light absorption enhancement due to the inclusion of Ag:SiO₂ nanoparticles for various shell thicknesses and core offsets. The core diameter and the position of the nanoparticle were kept constant at 40 nm and 21 nm above the

aluminum, respectively. The optimum diameter and position of Ag:SiO₂ were obtained from our previous work [34]. Enhanced scattering at lower material absorption is evident for a thinner shell (see Figure (b) and (c)). Light absorption was higher than the one without nanoparticles for all investigated shell thicknesses. Increased absorption with the embedment of nanoparticles is in agreement with many published works (i.e., [19,29,39,40]). Light absorption for the nanoparticle with 1 nm shell thickness is nearly three times (300% enhancement) the absorption without the nanoparticle. The absorption enhancement increases with core offset for a thinner shell.

High absorption enhancement originated from strong scattering and electric field localization around the nanoparticle [19,29,30]. Despite a similar trend, the slope of absorption enhancement with core offset was steeper for the thicker shell. Offsetting core position from concentric core-shell ($\delta=0$) to non-concentric or crescent-like nanoparticle ($\delta=\delta_{\max}$) increased the absorption enhancement by 2.01%, 6.75%, 12.4%, and 17.1% for shell thickness of 1 nm, 2 nm, 3 nm, and 4 nm, respectively. Higher absorption enhancement for thinner shells can be explained as a result of more considerable penetration of the electric field into the active layer leading to increasing photon absorption. The reduced enhancement slope for a thinner shell was related to a lower nominal offset that was equal to shell thickness. The obtained light absorption enhancement was found higher than that of in many previously published works, i.e., 106% [22], 150% [41], 127% [29], 160% [21], 198% [30], and 210% [34]. The excitation of Fano resonances made the obtained absorption enhancement higher in this work due to the use of asymmetric core-shell nanoparticles.

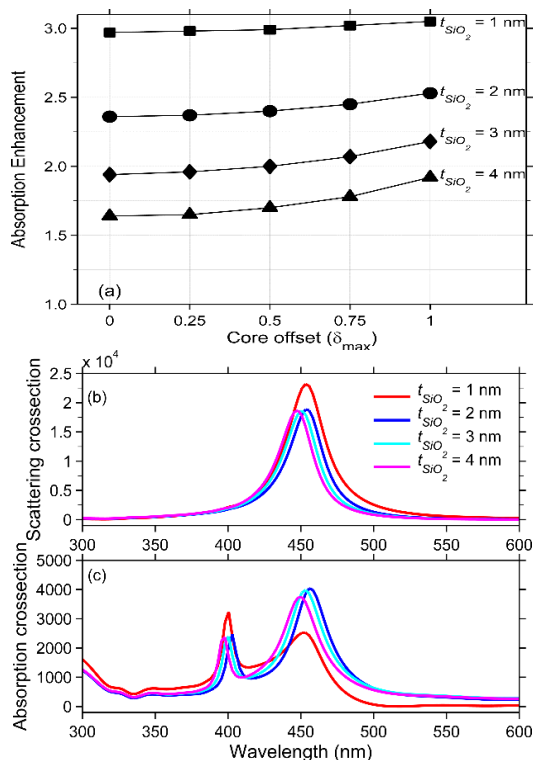


Fig. 2. (a) Light absorption enhancement as a function of Ag:SiO₂ nanoparticle core offset for different shell thickness, (b) scattering cross-section, and (c) absorption cross-section. The shell thickness is indicated in the graphs.

The scattering of core-shell nanoparticles with a core

diameter of 40 nm was nearly one order of magnitude higher than its absorption (See Figure 2(b) and 2(c)). The tendency of particles larger than 30 nm to scatter rather than to absorb is well known [8,42]. The particle scattering the light is more beneficial for solar cell applications. It implies that incoming incident light will be scattered around the nanoparticle to be absorbed in the active layer of an OSC instead of the nanoparticles themselves. The scattering peak of core-shell nanoparticles with a 1 nm shell was found higher and broader than others. The scattering and absorption for shell thickness 2 – 4 nm did not differ much. Stronger light confinement can explain the lower scattering for thicker shells at the interface of silver and SiO₂.

We calculated the electric field distribution around the core-shell nanoparticle to prove that the absorption enhancement is caused by stronger light localization and penetration into the active layer. The results are shown in Figure 3. A higher electric field is evident at the interface between the metal and the dielectric material. The black horizontal line in each subplot represents the interface between PEDOT: PSS – P3HT: PCBM. Due to a higher refractive index of P3HT: PCBM, electric field localization became stronger within this active layer. The decay of field intensity was quite slow so that the relatively high field on the order of $3 - 5 \cdot 10^9$ was distributed in the active layer. When light was concentrated within the active material, optical absorption increased proportionally to the square of the field enhancement factor [31].

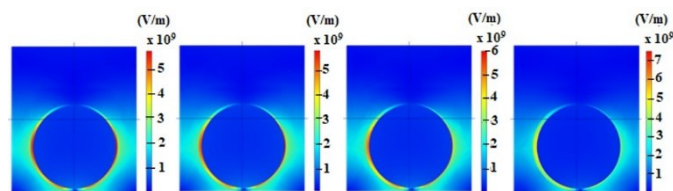


Fig. 3. (left–right) Distribution of electric field around Ag:SiO₂ nanoparticle for different core offsets, namely $0.25 \delta_{\max}$, $0.5 \delta_{\max}$, $0.75 \delta_{\max}$, and δ_{\max} .

The scale of the color bar in Figure 3 indicates the electric field distribution. The red (blue) colored area corresponds to a higher (lower) electric field. The localization of the light electric field is more substantial for a larger core offset. When the offset is larger, metal is almost in direct contact with the active layer resulting in a higher field localization and absorption in this layer. High electric field localization arises from Fano resonance excitation. For a thicker shell, fast decay of localized electric field at the interface of silver and SiO₂ shell does not reach the entire volume of the active layer. Therefore, light absorption enhancement decreases.

3.2. Effect of core offset angle

In the previous section, we have shown the effect of core offset on the light absorption enhancement in the active layer of an OSC. The offset was varied along the x-axis or horizontal direction. Further optimization was performed on the effect of Ag:SiO₂ core-shell scattering cross section by changing the offset orientation. Figure 4 shows the effect of core offset orientation. A dependence of absorption enhancement on the orientation angle was apparent. The minimum enhancement was obtained when the core of Ag:SiO₂ has shifted upward so that the distance between the silver core and aluminum

electrode increased. Whereas, the maximum enhancement was obtained when the silver core was shifted downward, approaching the aluminum electrode. When the offset was in the lateral direction, the enhancement was the same (i.e. rotationally symmetric) as expected. An additional explanation for the core-offset orientation is the nanoparticle scattering profile. Maximum absorption enhancement at a core offset angle of 270° (for the case where silica shell nano “crescent” facing downward) corresponds to a higher forward light scattering into the active layer. Higher electric field intensity inside the active layer allows a higher light absorption to produce excitons. Oppositely, at an angle of 90° (for the case where silica shell nano “crescent” facing upward) it causes light to be backscattered into PEDOT: PSS layer; therefore, light absorption in the active layer decreases.

The total change of absorption enhancement with core offset orientation was about 18.5%. The increase of the absorption enhancement with core offset orientation was determined by stronger electric field localization at the minimum distance between the silver core and the aluminum electrode. The effective back reflection was also expected when the silver core faced the aluminum electrode directly. The obtained absorption enhancement up to 345% was higher than that of reported in the literature [22,23,29,30,40,43]. In most of the works mentioned before, the nanoparticle was located at the interface of PEDOT: PSS - P3HT: PCBM, while in this work, the core-shell nanoparticle was deeper into the active layer. Nanoparticle embedding in the active layer may explain why light absorption enhancement was found higher in our investigation.

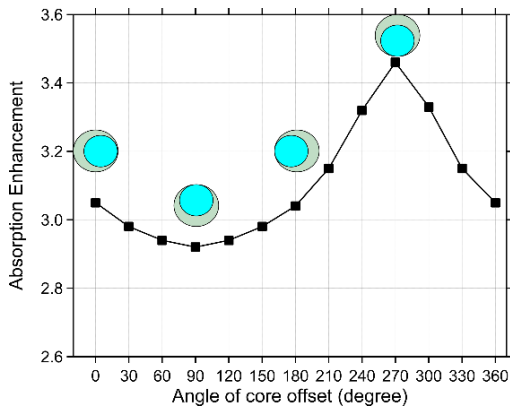


Fig. 4. Effect of Ag:SiO₂ nanoparticle core offset orientation on light absorption enhancement due to the inclusion in the active layer. The diameter of the silver core is 40 nm, while the shell thickness is 1 nm.

3.3. Effect of periodicity

Distance between neighboring nanoparticles or periodicity affects the light absorption enhancement (see Figure 5). Absorption enhancement decreased exponentially with the periodicity. The effect of periodicity originated from a more homogeneous distribution of the electric field in the active layer. The smaller the distance, the higher and the more homogeneously distributed the electric field in the active layer. Higher electric field resulted in increasing light absorption used to generate excitons. For periodicity above 400 nm, the effect of metal nanoparticles disappeared. The enhancement absorption was the same as the one without metal

nanoparticles.

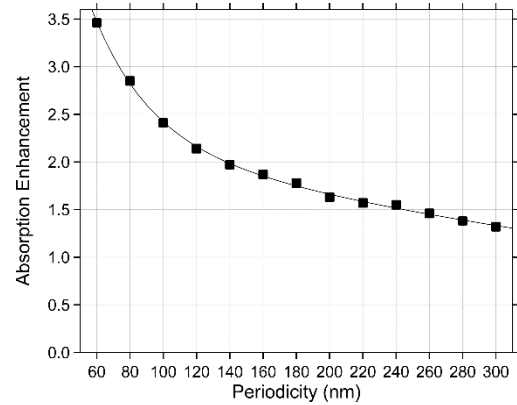


Fig. 5. Effect of Ag:SiO₂ nanoparticle periodicity on the absorption. The diameter of the silver core is 40 nm, while the shell thickness is 1 nm.

Increasing light absorption enhancement at smaller particle separation can be explained by increasing particle fill fraction in the active layer. Nanoparticles can be considered as nanoantennae collecting incident light from the sun and then scattering it into their surroundings while a significant fraction of light is localized around the nanoparticles [44]. The increase in nanoantennae corresponds directly to the scattering cross-sections of the nanoparticles. This result indicates the existence of the threshold fill fraction for the metal nanoparticles to be able to enhance light absorption in an organic solar cell. Below a specific value, the plasmonic effect becomes too weak to induce light absorption enhancement.

When the distance between nanoparticles increases, the electric field decays at the interface of the silver core, and SiO₂ cannot penetrate deeper into the active layer of OSC. In addition, oscillation resonance between neighboring particles is much stronger in the smaller separation distance. Resonance allows the efficient and mutual strengthening of the localized electric field around the nanoparticles. This interaction gets weaker when nanoparticles are too distant from each other. As a consequence, fewer photons are available to be absorbed to generate excitons in the active layer. A similar trend of decreased light absorption enhancement with periodicity has been reported before [30].

3.4. Effect of mismatch in vertical position

In the previous sections, we calculated light absorption enhancement for a periodic core-shell Ag:SiO₂ nanoparticle arrangement. We further investigated the effect of the imperfect alignment of the vertical position of the nanoparticles to mimic natural fabrication results. The distance between neighboring particles was kept constant at 60 nm. Figure 6 shows the dependency of absorption enhancement on the mismatch in the vertical position of neighboring particles. The position of the first nanoparticle was fixed at 21 nm above the aluminum electrode, while the position of the center of the neighbor particle was varied. The position of the first nanoparticle was obtained from the previous optimization step [30]. The largest mismatch was -49 nm when the nanoparticle was located at ITO – PEDOT: PSS interface. Zero mismatches is a condition when the second nanoparticle is at the same vertical position as the first. The maximum positive mismatch of +21 nm occurs

when the center of the second nanoparticle is at the interface of P3HT:PCBM – aluminum. The absorption enhancement is maximum when the mismatch is zero but it decreases again when the neighboring nanoparticle is closer to the aluminum electrode due to resonance mismatch. The mismatch of nanoparticle position affects resonance coupling between neighboring particles.

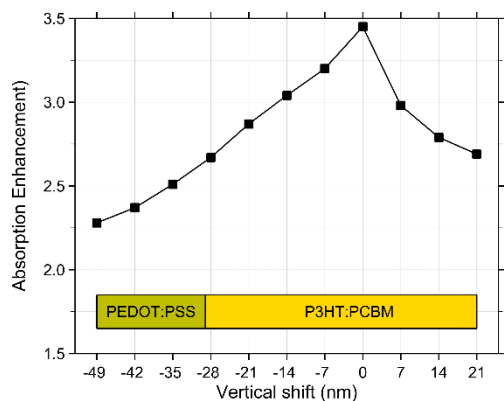


Fig. 6. Effect of the vertical shift of neighboring Ag:SiO₂ nanoparticle on the absorption enhancement of OSC.

Lower absorption enhancement when the second nanoparticle was in the PEDOT: PSS layer can be explained to originate from the difference in resonance wavelength. A lower refractive index of PEDOT caused a difference in resonance wavelength in PSS compared to in P3HT: PCBM. The different resonance wavelengths avoided efficient resonance coupling between the nanoparticles. When the second nanoparticle moved down into the active layer, resonance coupling increased; and absorption enhancement increased as well. The resonance coupling was maximum when the mismatch was zero because the resonance wavelength was the same for both nanoparticles due to exactly similar surrounding materials. The difference in resonance wavelength caused the decrease of absorption enhancement when the mismatch was positive as the second nanoparticle partially penetrated the aluminum electrode. Nanoparticle penetration shifted the resonance wavelength substantially, avoiding efficient resonance coupling between the nanoparticles.

The obtained absorption enhancement was above 225%, even at the largest mismatch. This result was much higher than the reported data for randomly distributed metal nanoparticles [45]. It was twice higher than that of the active layer's absorption without the embedded core-shell nanoparticle. The absorption enhancement gradually increased when vertical position mismatch decreased due to a higher overlap of the electric field scattered by both neighboring particles in the active layer.

To explain the mismatch effect, we calculated field distribution around neighboring nanoparticles and display it in Figure 7. Stronger light localization, and a more homogeneously distributed electric field are visible when the position mismatch is zero. Some fractions of electric field localization around the second nanoparticle lied in the PEDOT: PSS layer. The electric field in this layer did not contribute to exciton generation because it was not the active layer. When both nanoparticles' vertical position was parallel, the electric field in the active layer increased significantly. In addition, an

intense electric field in between the silver core and aluminum was generated due to the so-called lightning rod effect. The lightning rod effect explains why electrons and electric fields accumulated near sharp edges or between two closely separated metals. The absorption enhancement can also be partially explained due to the aluminum electrode's back reflection. Incident or scattered light approaching the aluminum electrode will be reflected into the active layer. Multiple passes of light through the OSC's active layer increase its absorption probability.

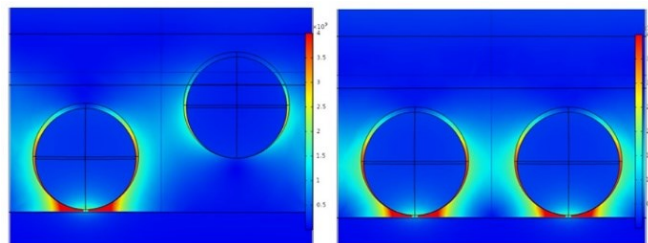


Fig. 7. Effect of the vertical shift of Ag:SiO₂ neighboring nanoparticle on the electric field distribution inside the OSC, (left) mismatch -21 nm, and (right) zero mismatch.

4. Conclusion

We have shown the dependency of the absorption enhancement of organic solar cells with embedded Ag:SiO₂ core-shell nanoparticles on the shell thickness, core offset, core offset orientation, periodicity, and vertical position mismatch. The absorption enhancement increased with core offset and decreased with shell thickness. It depended on the core offset, and the absorption enhancement changed with the offset orientation angle. The maximum absorption enhancement was obtained for a core offset angle of 270°. The absorption enhancement decreased exponentially with the distance and reached the enhancement without nanoparticles when periodicity exceeded 400 nm. The absorption enhancement was found maximum when there was no vertical mismatch in the position of neighboring particles. At optimized conditions, an absorption enhancement of 345% could be obtained. The obtained enhancement was higher than the values as reported in the literature. Asymmetric core-shell nanoparticles were found to be very suitable for achieving a higher absorption enhancement. High absorption enhancement will benefit the realization of low-cost and high-efficiency organic solar cells.

Acknowledgments

The authors thank Universitas Andalas for funding this research with contract No. T/123/UN.16.17 /PT.01.03/Energi-RPT/2022.

References

1. M. B. Askari, *Introduction to Organic Solar Cells*, Sustainable Energy 2(3) (2014) 85-90.
2. L. X. Chen, *Organic Solar Cells: Recent Progress and Challenges*, ACS Energy Lett. 4 (2019) 2537–2539.
3. S. M. Falke, C. A. Rozzi, D. Brida, M. Maiuri, M. Amato, E. Sommer, et

- al., *Coherent ultrafast charge transfer in an organic photovoltaic blend*, Science 344(6187) (2014) 1001-1005.
4. C. E. Small, S.-W. Tsang, S. Chen, S. Baek, C. M. Amb, J. Subbiah, et al., *Loss Mechanisms in Thick-Film Low-Bandgap Polymer Solar Cells*, Adv. Energy Mater. 3(7) (2013) 909-916.
 5. C. J. Brabec, S. Gowrisanker, J. J. M. Halls, D. Laird, S. Jia, and S. P. Williams, *Polymer–Fullerene Bulk-Heterojunction Solar Cells*, Adv. Mater. 22(34) (2010) 3839-3856.
 6. H. Hoppe and N. S. Sariciftci, *Organic solar cells: An overview*, J. Mater. Res. 19 (2004) 1924–1945.
 7. T. Upreti, Y. Wang, H. Zhang, D. Scheunemann, F. Gao, and M. Kemerink, *Experimentally Validated Hopping-Transport Model for Energetically Disordered Organic Semiconductors*, Phys. Rev. Appl. 12 (2019) 064039.
 8. S. Ahn, D. Rourke, and W. Park, *Plasmonic nanostructures for organic photovoltaic devices*, J. Opt. 18 (2016) 033001.
 9. Z. Tang, W. Tress, and O. Inganäs, *Light trapping in thin film organic solar cells*, Mater. Today 17 (2014) 8.
 10. C. Cho, H. Kim, S. Jeong, Se-WoongBaek, J.-W. Seo, D. Han, et al., *Random and V-groove texturing for efficient light trapping in organic photovoltaic cells*, Sol. Energy Mater. Sol. Cells 115 (2013) 36–41.
 11. D. H. Wang, D.-G. Choi, K.-J. Lee, J.-H. Jeong, S. H. Jeon, O. O. Park, et al., *Effect of the ordered 2D-dot nano-patterned anode for polymer solar cells*, Org. Electron. 11(2) (2010) 285-290.
 12. Y. Park, J. Berger, Z. Tang, L. Müller-Meskamp, A. F. Lasagni, K. Vandewal, et al., *Flexible, light trapping substrates for organic photovoltaics*, Appl. Phys. Lett. 109 (2016) 093301.
 13. D.-H. Ko, J. R. Tumbleston, L. Zhang, S. Williams, J. M. DeSimone, R. Lopez, et al., *Photonic Crystal Geometry for Organic Solar Cells*, Nano Lett. 9(7) (2009) 2742–2746.
 14. D. Duché, C. Masclaux, J. L. Rouzo, and C. Gourgon, *Photonic crystals for improving light absorption in organic solar cells*, J. Appl. Physics 117 (2015) 053108.
 15. Z. Hu, J. Zhang, and Y. Zhao, *Effect of textured electrodes with light-trapping on performance of polymer solar cells*, J. Appl. Physics 111 (2012) 104516.
 16. K. Tvingstedt, S. D. Zilio, O. Inganäs, and M. Tormen, *Trapping light with micro lenses in thin film organic photovoltaic cells*, Opt. Express 16(26) (2008) 21608-21615.
 17. J. D. Myers, W. Cao, V. Cassidy, S.-H. Eom, R. Zhou, L. Yang, et al., *A universal optical approach to enhancing efficiency of organic-based photovoltaic devices*, Energy Environ. Sci. 5 (2012) 6900-6904.
 18. H. A. Atwater and A. Polman, *Plasmonics for improved photovoltaic devices*, Nat. Mater. 9 (2010) 205–213.
 19. K. A. Catchpole and A. Polman, *Plasmonic solar cells*, Opt. Express 16(26) (2008) 21793–21800.
 20. A. Phengdaam, S. Nootchanat, R. Ishikawa, C. Lertvachirapaiboon, K. Shinbo, K. Kato, et al., *Improvement of organic solar cell performance by multiple plasmonic excitations using mixed-silver nanoprisms*, J. Sci.: Adv. Mater. Devices 6(2) (2021) 264-270.
 21. F. Liu, W. Xie, Q. Xu, Y. Liu, K. Cui, X. Feng, et al., *Plasmonic Enhanced Optical Absorption in Organic Solar Cells With Metallic Nanoparticles*, IEEE Photonics J. 5(4) (2013) 8400509.
 22. D. Qu, F. Liu, Y. Huang, W. Xie, and Q. Xu, *Mechanism of optical absorption enhancement in thin film organic solar cells with plasmonic metal nanoparticles*, Opt. Express 19(24) (2011) 24795-24803.
 23. C. C. D. Wang, W. C. H. Choy, C. Duan, D. D. S. Fung, W. E. I. Sha, F.-X. Xie, et al., *Optical and electrical effects of gold nanoparticles in the active layer of polymer solar cells*, J. Mater. Chem. 22 (2012) 1206-1211.
 24. S. Manzhos, G. Giorgi, J. Lüder, and M. Ihara, *Modeling of plasmonic properties of nanostructures for next generation solar cells and beyond*, Adv. in Phys.: X 6(1) (2021) 1908848.
 25. D. Kozanoglu, D. H. Apaydin, A. Cirpan, and E. N. Esenturk, *Power conversion efficiency enhancement of organic solar cells by addition of gold nanostars, nanorods, and nanospheres*, Org. Electron. 14(7) (2013) 1720-1727.
 26. A. Rana, N. Gupta, A. Lochan, G. D. Sharma, S. Chand, M. Kumar, et al., *Charge carrier dynamics and surface plasmon interaction in gold nanorod-blended organic solar cell*, J. Appl. Phys. 120 (2016) 063102.
 27. P. Yu, Y. Yao, J. Wu, X. Niu, A. L. Rogach, and Z. Wang, *Effects of Plasmonic Metal Core -Dielectric Shell Nanoparticles on the Broadband Light Absorption Enhancement in Thin Film Solar Cells*, Sci. Rep. 7 (2017) 7696.
 28. J. You, K. Leonard, Y. Takahashi, H. Yonemura, and S. Yamada, *Effects of silver nanoparticles with different sizes on photochemical responses of polythiophene–fullerene thin films*, Phys. Chem. Chem. Phys. 16 (2014) 1166-1173.
 29. K. N'Konou, L. Peres, and P. Torchio, *Optical Absorption Modeling of Plasmonic Organic Solar Cells Embedding Silica-Coated Silver Nanospheres*, Plasmonics 13 (2018) 297–303.
 30. I. Perdana and M. Muldarisnur, *Optimization of Ag-SiO₂ core-shell nanoparticles arrangement for light absorption enhancement in organic solar cells*, the National Seminar of Physics (SNF), Jakarta, Indonesia, 2020, 030008.
 31. H. Shen, P. Bienstman, and B. Maes, *Plasmonic absorption enhancement in organic solar cells with thin active layers*, J. Appl. Phys. 106 (2009) 073109.
 32. A. Chafidz, A. R. Afandi, B. M. Rosa, J. Suhartono, P. Hidayat, and H. Junaedi, *Production of silver nanoparticles via green method using banana raja peel extract as a reducing agent*, Commun. Sci. Technol. 5(2) (2020) 112–118.
 33. L. M. Quynh, H. V. Huy, N. D. Thien, L. T. C. Van, and L. V. Dung, *Synthesis of Si/SiO₂ core/shell fluorescent submicron-spheres for monitoring the accumulation of colloidal silica during the growth of diatom Chaetoceros sp.*, Commun. Sci. Technol. 7(1) (2022) 1–7.
 34. F. Fahendri, I. Perdana, Z. Abdullah, and M. Muldarisnur, *Enhancement of Light Absorption in the Active Layer of Organic Solar Cells using Ag:SiO₂ Core-Shell Nanoparticles* JPPIPA 8(6) (2022)
 35. S. Humphries, *Finite-element methods for electromagnetics*. Albuquerque, New Mexico: CRC Press, 2010.
 36. J.-M. Jin, *The Finite Element Method in Electromagnetics* 3 ed. New York: Wiley-IEEE Press, 2014.
 37. G. Chidichimo and L. Filippelli, *Organic Solar Cells: Problems and Perspectives*, Int. J. Photoenergy 2010 (2010) 123534.
 38. American Society for Testing and Materials, *Standard tables for terrestrial solar spectral irradiance at air mass 1.5 for a 37° tilted surface*. Philadelphia, PA: American Society for Testing and Materials, 1987.
 39. D. H. Wang, D. Y. Kim, K. W. Choi, J. H. Seo, S. H. Im, J. H. Park, et al., *Enhancement of Donor–Acceptor Polymer Bulk Heterojunction Solar Cell Power Conversion Efficiencies by Addition of Au Nanoparticles*, Angew. Chemie Int. Ed. 50(24) (2011) 5519-5523.
 40. D. H. Wang, J. K. Kim, G.-H. Lim, K. H. Park, O. O. Park, B. Lim, et al., *Enhanced light harvesting in bulk heterojunction photovoltaic devices with shape-controlled Ag nanomaterials: Ag nanoparticles versus Ag nanoplates*, RSC Adv. 2 (2012) 7268-7272.
 41. D. Duche, P. Torchio, L. Escoubas, F. Monestier, J.-J. Simon, F. Flory, et al., *Improving light absorption in organic solar cells by plasmonic contribution*, Sol. Energy Mater. Sol. Cells 93(8) (2009) 1377-1382.
 42. L. Feng, M. Niu, Z. Wen, and X. Hao, *Recent Advances of Plasmonic Organic Solar Cells: Photophysical Investigations*, Polymers 10(123)

- (2018) 1-33.
43. G. D. Spyropoulos, M. M. Stylianakis, E. Stratakis, and E. Kymakis, *Organic bulk heterojunction photovoltaic devices with surfactant-free Au nanoparticles embedded in the active layer*, *Appl. Phys. Lett.* 100 (2012) 213904.
44. A. P. Amalathas and M. M. Alkaisi, *Nanostructures for Light Trapping in Thin Film Solar Cells*, *Micromachines* 10(619) (2019) 1-18.
45. M. Piralaee, Z. Ebrahimpour, and A. Asgari, *The improved performance of BHJ organic solar cells by random dispersed metal nanoparticles through the active layer*, *Curr. Appl. Phys.* 20 (2020) 531-537.